Non-cascaded Dynamic Inversion Design for Quadrotor Position Control with L1 Augmentation

Jian Wang, Florian Holzapfel

Institute of Flight System Dynamics, TU München, Germany, 85748

Enric Xargay, Naira Hovakimyan

University of Illinois at Urbana-Champaign, Urbana, IL 61801

Abstract This paper presents a position control design for quadrotors, aiming to exploit the physical capability and maximize the full control bandwidth of the quadrotor. A novel non-cascaded dynamic inversion design is used for the baseline control, augmented by an L1 adaptive control in the rotational dynamics. A new implementation technique is developed in the linear reference model and error controller; so that without causing any inconsistency, nonlinear states can be limited to their physical constraints. The L1 adaptive control is derived to compensate plant uncertainties like inversion error, disturbances, and parameter changes. Simulation and experiment tests have been performed to verify the effectiveness of the designs and the validity of the approach.

Nomenclature

B	Body frame
W	World frame, a leveled frame with user-defined x-axis deduced from NED frame
k_n	Propeller force constant
k_m	Propeller moment constant
$F_{prop,i}$	Force produced by ith propeller
$M_{prop,i}$	Torque produced by ith propeller
$\vec{\boldsymbol{r}}$	Position vector of the C.G, resolved in frame W

$\vec{\boldsymbol{v}}$	Velocity vector of the C.G, time derivative taken in frame W, resolved in frame W
$\vec{\boldsymbol{a}}$	Acceleration vector of the C.G, time derivative taken in frame W, resolved in frame W
$\dot{\vec{\boldsymbol{a}}}$	Acceleration derivative vector of the C.G, time derivative taken in frame W, resolved in frame W
$\boldsymbol{M}_{WB}$	Rotation matrix, from frame B to frame W
$\vec{\boldsymbol{\omega}}$	$=[p \quad q \quad r]^T$, angular rates around x, y and z axis of frame B
$\vec{\boldsymbol{F}}_W$	Force vector in frame W
T	Total thrust, acting on the z axis of Frame B
$\vec{\boldsymbol{f}}_B$	$=[f_x \quad f_y \quad f_z]^T$, specific force vector denoted in frame B
$\vec{\boldsymbol{M}}$	$=[L \quad M \quad N]^T$, moments around x, y and z axis of frame B
$\boldsymbol{J}$	Moment of inertia tensor with respect to the C.G
$\vec{\boldsymbol{g}}$	$=[0 \quad 0 \quad g]^T$, gravity vector
$\boldsymbol{I}$	$=\begin{bmatrix}1 & 0 & 0\\ 0 & 1 & 0\\ 0 & 0 & 1\end{bmatrix}$, identity matrix
$\boldsymbol{n_i}$	$\boldsymbol{i} = 1,2,3,4$, normalized rotor rotation speeds

1. Introduction

Multirotor platforms have gained increasing interest as a research platform, due to its VTOL and hovering capabilities, easy construction and steering principle, as well as high maneuverability. The flight performance of conventional position controllers is relatively low. This can be observed by the performance difference between a quadrotor flown autonomously and one piloted by an experienced pilot. The work in [1, 2], with the help of the Vicon system [3], they made highly aggressive maneuvers, however switching controllers are used to fulfill one trajectory, i.e., only attitude or rate controller is used during the aerobatic segment of the trajectory and afterwards hover control is activated to desired position. Design of one position controller to maximize and fully exploit the control bandwidth is of particular interest of the author.

One well-known inherent property of the multi-rotor position dynamics is of non-triangular form. The usual control inputs before the control allocation are the total thrust and three axis moments. At near hovering condition, from the total thrust to z-axis position there are two system orders (integrators), while from moment to x-y-axis position there are four system orders. However, they are strongly coupled, esp. at large angle high speed flight conditions.

In the companion paper [4], through comparison of 7 structure designs using backstepping and dynamic inversion, non-cascaded dynamic inversion design is concluded to give the maximum control bandwidth, however, it is not applicable to system of non-triangular form. Previous efforts on non-cascaded design include

the quasi-steady height assumption approach [5] and dynamic extension assumption in [6]. In [5], the height control and x-y-axis position control were separated, and quasi-steady height control was assumed in order to decouple the x-y-position dynamics. However, for high angle high speed flight, height is often compromised to gain more force in the leveled plane. In [6], though only linearly approximated inversion was derived, there is elegant modification: the thrust dynamics is artificially extended by two more system order so that the position dynamics is of triangular form. Naturally, this will slow down the thrust dynamics a little, but the overall control bandwidth is increased. A chain is no stronger than its weakest link. For the quadrotor, the moment dynamics are relatively slower than thrust dynamics, thus the weak link of the position control. The author also developed three other designs of position controllers in [7, 8, 9], and they are compared with the new design to examine the advantages.

In this paper, a thrust dynamic extension is used to transform the system into triangular form. Then an exact dynamic inversion approach with non-cascaded structure can be derived. Pseudo Control Hedging (PCH) [10] is also implemented. The detailed derivations are given in the section 2. The L1 adaptive control [11] of piecewise constant type is augmented to compensate the plant uncertainties. Its derivation is given in section 3. Finally, this control design is verified in the simulation and flight tests. The results and comparisons with other position control designs are presented in section 4 and followed by the conclusion in the last section.

2. Exact Dynamic Inversion Design with Non-cascaded Structure

Nonlinear dynamic inversion control [12] normally consists of three major blocks:

1. Reference model: to generate smooth enough trajectory for the vehicle.
2. Linear error controller: to account for inversion error and disturbance.
3. Dynamic inversion: to transform the nonlinear plant to an equivalently linear one.

In the following sections, these three parts is designed and illustrated in details. The yaw axis has separated control as it is inherently decoupled from the position dynamics. Control allocation and PCH are presented as well. The following figure can give an overview of the whole control design, where the L1 augmentation loop is presented in section 3.

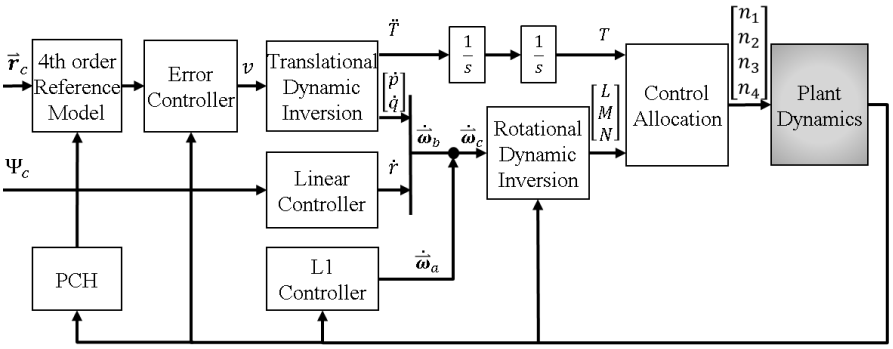

Fig. 1. Overview of the control design

2.1 Extended Translational Dynamics

For small UAVs, a local leveled frame is often used as the inertial frame. In this case, the World frame is defined, which is the NED frame rotated around the vertical axis by a user defined heading angle. The desired output is the position in the W frame. The position dynamic equation is extended to be actuated by the thrust 2nd derivative and angular accelerations.

The following linear state vector is used for the translational control design,

$$\boldsymbol{X} = [\vec{\boldsymbol{r}} \quad \vec{\boldsymbol{v}} \quad \vec{\boldsymbol{a}} \quad \dot{\vec{\boldsymbol{a}}}]^T \tag{1}$$

The newton's 2nd law is used to derive the translational dynamic equation,

$$\vec{\boldsymbol{F}}_W = m \cdot \dot{\vec{\boldsymbol{v}}} = m \cdot \boldsymbol{M}_{WB} \cdot (\vec{\boldsymbol{f}}_{prop,B} + \vec{\boldsymbol{f}}_{aero,B}) + m \cdot \vec{\boldsymbol{g}} \tag{2}$$

The force $\vec{\boldsymbol{f}}_{prop,B}$ is the thrust vector generated by the propeller normalized by the mass and can be assumed to be aligned with the z-axis of the Body frame. The normalized aerodynamic force $\vec{\boldsymbol{f}}_{aero,B}$ mainly includes drag and wind disturbances.

In conventional control design with attitude as control state, the aerodynamic force is often neglected. That is fine in indoor environment, but they are not negligible in outdoor environment or at high speed flight situation. In this design, as acceleration $\vec{\boldsymbol{a}}$ is used as control state which can be measured by the accelerometer, the aerodynamic force is embedded and feedbacked to the error controller. The accelerometer measures the specific force $\vec{\boldsymbol{f}}_B$ in the Body frame, which is the sum of propeller force and aerodynamic force in Eq. (2).

$$\vec{\boldsymbol{f}}_B = \begin{bmatrix} f_x \\ f_y \\ f_z \end{bmatrix} = \left(\begin{bmatrix} 0 \\ 0 \\ -\frac{T}{m} \end{bmatrix} + \vec{\boldsymbol{f}}_{aero,B} \right) \tag{3}$$

As we will further extend the translational dynamics to the angular acceleration, Eq. (2) needs to be further differentiated twice. The derivative of the aerodynamics force has to be dumped as there is neither measurement nor analytical expression for it. Nevertheless, it is already better than the attitude feedback case. And the inversion error due to this will be compensated by the error controller.

Dividing both sides of Eq. (2) by the mass and replacing the $\vec{\boldsymbol{f}}_{prop,B}$ by the normalized thrust, we have,

$$\dot{\vec{\boldsymbol{v}}} = \boldsymbol{M}_{WB} \cdot \begin{bmatrix} f_x \\ f_y \\ f_z \end{bmatrix} + \begin{bmatrix} 0 \\ 0 \\ g \end{bmatrix} \approx \boldsymbol{M}_{WB} \cdot \begin{bmatrix} 0 \\ 0 \\ -\frac{T}{m} \end{bmatrix} + \begin{bmatrix} 0 \\ 0 \\ g \end{bmatrix} \tag{4}$$

Further differentiate the above equation,

$$\ddot{\vec{\boldsymbol{v}}} = \dot{\vec{\boldsymbol{a}}} = \dot{\boldsymbol{M}}_{WB} \cdot \begin{bmatrix} 0 \\ 0 \\ -\frac{T}{m} \end{bmatrix} + \boldsymbol{M}_{WB} \cdot \begin{bmatrix} 0 \\ 0 \\ -\frac{\dot{T}}{m} \end{bmatrix} \tag{5}$$

Using Euler differentiation rule, we have

$$\dot{\boldsymbol{M}}_{WB} = \boldsymbol{M}_{WB} \cdot S(\vec{\boldsymbol{\omega}}) = \boldsymbol{M}_{WB} \begin{bmatrix} 0 & -r & q \\ r & 0 & -p \\ -q & p & 0 \end{bmatrix} \tag{6}$$

Inserting Eq. (6) into Eq. (5),

$$\dot{\vec{\boldsymbol{a}}} = \boldsymbol{M}_{WB} \cdot \begin{bmatrix} 0 & -r & q \\ r & 0 & -p \\ -q & p & 0 \end{bmatrix} \begin{bmatrix} 0 \\ 0 \\ -\frac{T}{m} \end{bmatrix} + \boldsymbol{M}_{WB} \cdot \begin{bmatrix} 0 \\ 0 \\ -\frac{\dot{T}}{m} \end{bmatrix} \tag{7}$$

$$= \boldsymbol{M}_{WB} \cdot m^{-1} \left(\begin{bmatrix} -Tq \\ Tp \\ -T \end{bmatrix} + \begin{bmatrix} 0 \\ 0 \\ -\dot{T} \end{bmatrix} \right) \tag{8}$$

$$= \boldsymbol{M}_{WB} \cdot m^{-1} \begin{bmatrix} 0 & -T & 0 \\ T & 0 & 0 \\ 0 & 0 & -1 \end{bmatrix} \begin{bmatrix} p \\ q \\ \dot{T} \end{bmatrix} \tag{9}$$

Differentiating it one more time, angular accelerations appear explicitly in the equation.

$$\ddot{\vec{a}} = \boldsymbol{M}_{WB}\begin{bmatrix} 0 & -r & q \\ r & 0 & -p \\ -q & p & 0 \end{bmatrix} \cdot m^{-1}\begin{bmatrix} 0 & -T & 0 \\ T & 0 & 0 \\ 0 & 0 & -1 \end{bmatrix}\begin{bmatrix} p \\ q \\ \dot{T} \end{bmatrix} +$$

$$\boldsymbol{M}_{WB} \cdot m^{-1}\begin{bmatrix} 0 & -\dot{T} & 0 \\ \dot{T} & 0 & 0 \\ 0 & 0 & 0 \end{bmatrix}\begin{bmatrix} p \\ q \\ \dot{T} \end{bmatrix} + \boldsymbol{M}_{WB} \cdot m^{-1}\begin{bmatrix} 0 & -T & 0 \\ T & 0 & 0 \\ 0 & 0 & -1 \end{bmatrix}\begin{bmatrix} \dot{p} \\ \dot{q} \\ \ddot{T} \end{bmatrix} \tag{10}$$

$$= \boldsymbol{M}_{WB} \cdot m^{-1}\left(\begin{bmatrix} -Tr & 0 & -q \\ 0 & -Tr & p \\ Tp & Tq & 0 \end{bmatrix} + \begin{bmatrix} 0 & -\dot{T} & 0 \\ \dot{T} & 0 & 0 \\ 0 & 0 & 0 \end{bmatrix}\right)\begin{bmatrix} p \\ q \\ \dot{T} \end{bmatrix} +$$

$$\boldsymbol{M}_{WB} \cdot m^{-1}\begin{bmatrix} 0 & -T & 0 \\ T & 0 & 0 \\ 0 & 0 & -1 \end{bmatrix}\begin{bmatrix} \dot{p} \\ \dot{q} \\ \ddot{T} \end{bmatrix} \tag{11}$$

$$= \boldsymbol{M}_{WB} \cdot m^{-1}\begin{bmatrix} -Trp - 2\dot{T}q \\ -Trq + 2\dot{T}p \\ Tp^2 + Tq^2 \end{bmatrix} + \boldsymbol{M}_{WB} \cdot m^{-1}\begin{bmatrix} 0 & -T & 0 \\ T & 0 & 0 \\ 0 & 0 & -1 \end{bmatrix}\begin{bmatrix} \dot{p} \\ \dot{q} \\ \ddot{T} \end{bmatrix} \tag{12}$$

$$= \boldsymbol{M}_{WB} \cdot m^{-1}\left(\begin{bmatrix} -Trp - 2\dot{T}q \\ -Trq + 2\dot{T}p \\ Tp^2 + Tq^2 \end{bmatrix} + \begin{bmatrix} 0 & -T & 0 \\ T & 0 & 0 \\ 0 & 0 & -1 \end{bmatrix}\begin{bmatrix} \dot{p} \\ \dot{q} \\ \ddot{T} \end{bmatrix}\right) \tag{13}$$

As we can see, not only the angular acceleration appears explicitly, but also the thrust has been differentiated twice. That's the analytical reason why we need to extend the thrust dynamics to its second derivative. With the derived dynamic equation, they can be inverted and derive the control commands in section 2.4.

2.2 Reference Model with Nonlinear State Limitations

The reference model has two main functions: 1. Generate smooth enough signal for the plant to follow, or generate the reference dynamics based on given requirement; 2. consider the physical plant constraints and limit the reference commands.

To generate smooth enough reference signals, a 4th order reference model is used (same dynamic order as the plant excluding actuator dynamics). The limitations of the reference commands are not so simple. Two challenges arise while imposing the limits: 1. the easiest way to impose the limits is to limit the integrator states, which is fine with slow reference dynamics but will cause inconsistency between the states as soon as the limits are reached. This happens much more often when high bandwidth high system order signals are demanded; 2. The physical

constraints are normally on the nonlinear states, so it is not accurate to impose them on the linear reference states.

In this section, a novel and simple reference structure is designed to overcome both challenges mentioned above. Let's first look at a conventional 4th order low pass filter. The dynamic equations in Laplace domain and time domain are

$$\begin{cases} \vec{\boldsymbol{r}}_r = \frac{k_0}{s^4+k_3s^3+k_2s^2+k_1s+k_0}\vec{\boldsymbol{r}}_c \\ \dddot{\vec{\boldsymbol{r}}}_r = k_0(\vec{\boldsymbol{r}}_c - \vec{\boldsymbol{r}}_r) - k_1\dot{\vec{\boldsymbol{r}}}_r - k_2\ddot{\vec{\boldsymbol{r}}}_r - k_3\dddot{\vec{\boldsymbol{r}}}_r \end{cases} \tag{14}$$

The parameters can be determined by pole placement method. All four poles are assigned to the same value $-\omega$, so that the reference error dynamics are critically damped. And also the gain tuning is reduced to one parameter (ω) tuning. For stability consideration, the reference dynamics should not be faster than the error dynamics. To have maximum control bandwidth, the parameter is tuned to be the same as that in the error dynamics. The gains can be assigned according to the characteristic equation in the Laplace domain.

$$s^4 + k_3s^3 + k_2s^2 + k_1s + k_0 = s^4 + 4\omega s^3 + 6\omega^2 s^2 + 4\omega^3 s + \omega^4 \tag{15}$$

The reference model can be considered as a problem of controlling a linear 4th order system (an integrator chain). The control law is in Eq. (14) and can be rewritten in the following form,

$$\dddot{\vec{\boldsymbol{r}}}_r = k_3\left\{\underbrace{\frac{k_2}{k_3}\left\{\underbrace{\frac{k_1}{k_2}\left[\underbrace{\frac{k_0}{k_1}(\vec{\boldsymbol{r}}_c - \vec{\boldsymbol{r}}_r)}_{\vec{\boldsymbol{v}}_c} - \dot{\vec{\boldsymbol{r}}}_r\right]}_{\vec{\boldsymbol{a}}_c} - \ddot{\vec{\boldsymbol{r}}}_r\right\}}_{\dot{\vec{\boldsymbol{a}}}_c} - \dddot{\vec{\boldsymbol{r}}}_r\right\} \tag{16}$$

Break the Eq. (16) down, we have,

$$\begin{cases} \vec{\boldsymbol{v}}_c = \frac{k_0}{k_1}(\vec{\boldsymbol{r}}_c - \vec{\boldsymbol{r}}_r) \\ \vec{\boldsymbol{a}}_c = \frac{k_1}{k_2}(\vec{\boldsymbol{v}}_c - \vec{\boldsymbol{v}}_r) \\ \dot{\vec{\boldsymbol{a}}}_c = \frac{k_2}{k_3}(\vec{\boldsymbol{a}}_c - \vec{\boldsymbol{a}}_r) \\ \ddot{\vec{\boldsymbol{a}}}_c = k_3(\dot{\vec{\boldsymbol{a}}}_c - \dot{\vec{\boldsymbol{a}}}_r) \end{cases} \tag{17}$$

The control law appears to be four cascaded linear 1st order control loops, but the feedback gains are still designed according to the non-cascaded control law as in Eq. (15), so the system bandwidth is not sacrificed by the apparent cascaded loops. With the above transformation, the state limits can be imposed on the

commands, meaning only the maximum allowable state is commanded to the next loop. In this way, we end up with a pure integrator chain without any forced state limits. The implementation structure is,

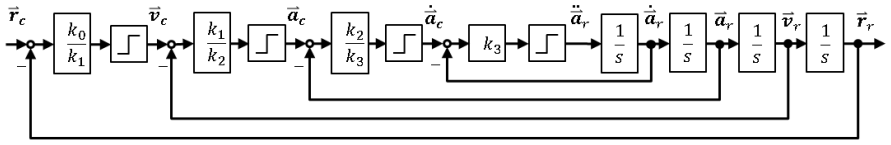

Fig. 2. 4th order low pass filter with linear state limitation

This only builds up the structure to impose linear state limits; however, the quadrotor have the physical constraints on the nonlinear states:

1. The maximum speed, in our case, is about 10m/s.
2. The maximum total thrust, depending on the propellers and motors. In our case, it is around 14N.
3. The maximum angular rate, limited by the gyroscope sensor range. In our case, it is 400°/s.
4. The maximum angular accelerations, limited by the max moments. In our case, the pitching and rolling moments are about 0.6 Nm, while the yawing moment is 0.1Nm.

The dynamic inversion idea can be also applied here to impose the nonlinear state constraints. The limitation block of each 'control loop' have to be modified, first the nonlinear state (which has physical constraints) is computed from the linear one and set the limits, then invert the limited nonlinear state back the linear state. The modifications on the above structure are illustrated as follows,

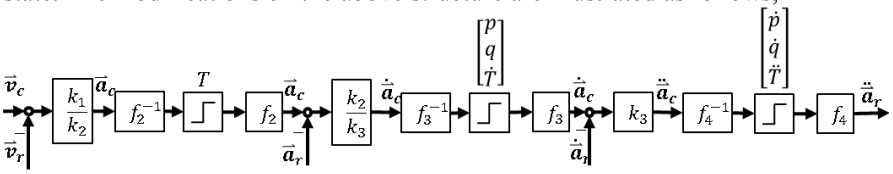

Fig. 3. Nonlinear state conversion and limitations in the reference model

Regarding the constraint 1, both $\vec{\boldsymbol{r}}_{\boldsymbol{c}}$ and $\vec{\boldsymbol{v}}_{\boldsymbol{c}}$ can be directly limited without any conversions.

Regarding the constraint 2, $\vec{\boldsymbol{a}}_{\boldsymbol{c}}$ is converted to thrust by inverting Eq. (4). Then the thrust is limited and converted back to $\vec{\boldsymbol{a}}_{\boldsymbol{c}}$ using Eq. (4).

$$T = \boldsymbol{M}_{BW}(3,:) \cdot \{\vec{\boldsymbol{a}}_{\boldsymbol{c}} - [0 \quad 0 \quad g]^T\} \tag{18}$$

Regarding the constraint 3, the $\dot{\vec{\boldsymbol{a}}}_{\boldsymbol{c}}$ is converted to pitch & roll rate and thrust derivative by inverting Eq. (9),

$$\begin{bmatrix} p \\ q \\ \dot{T} \end{bmatrix}_c = \begin{bmatrix} 0 & T^{-1} & 0 \\ -T^{-1} & 0 & 0 \\ 0 & 0 & -1 \end{bmatrix} \boldsymbol{M}_{BW} m \dddot{\boldsymbol{a}}_{\boldsymbol{c}} \tag{19}$$

After the angular rate is limited to the maximum gyro range, they are converted back. The thrust derivative doesn't have any constraint.

Regarding the constraint 4, the 'feedforward control' $\dddot{\boldsymbol{a}}_c$ is converted to pitch & roll rate accelerations and thrust 2nd derivative by inverting Eq. (13),

$$\begin{bmatrix} \dot{p} \\ \dot{q} \\ \ddot{T} \end{bmatrix} = \begin{bmatrix} 0 & T^{-1} & 0 \\ -T^{-1} & 0 & 0 \\ 0 & 0 & -1 \end{bmatrix} \left(\boldsymbol{M}_{BW} m \ddot{\boldsymbol{a}}_c - \begin{bmatrix} -Trp - 2\dot{T}q \\ -Trq + 2\dot{T}p \\ Tp^2 + Tq^2 \end{bmatrix} \right) \tag{20}$$

Then the resulting pitch and roll rate accelerations are limited based on the actuator constraints. Afterwards the limited states are converted back to $\dddot{\boldsymbol{a}}_r$ using Eq. (13). The thrust 2nd derivative doesn't have any constraints.

In the inversion equations above, there is some nonlinear state information needed. They are not the real state but the reference state so they should be taken or computed from 'the reference plant', i.e. the integrator chain. The reference azimuth angle can't be determined from the integrator chain. However, due to the symmetric geometry of quadrotors, the physical constraints in x-y-axis of the body frame are symmetric. So the reference azimuth angle can be regarded as zero when performing the inversion equations.

Among the nonlinear reference state, the reference rotation matrix $\boldsymbol{M}_{WB,r}$ needs a bit more effort to compute. With the azimuth angle set to be zero, it can be expressed by the pitch and bank angles,

$$\boldsymbol{M}_{WB,r} = \begin{bmatrix} \cos\Theta & \sin\Phi\sin\Theta & \cos\Phi\sin\Theta \\ 0 & \cos\Phi & \sin\Phi \\ -\sin\Theta & \sin\Phi\cos\Theta & \cos\Phi\cos\Theta \end{bmatrix} \tag{21}$$

The translational dynamic equation in Eq. (4) can be rewritten as,

$$\begin{bmatrix} a_x \\ a_y \\ a_z \end{bmatrix}_{W,r} = \boldsymbol{M}_{WB,r} \cdot \begin{bmatrix} 0 \\ 0 \\ f_z \end{bmatrix} + \begin{bmatrix} 0 \\ 0 \\ g \end{bmatrix} \tag{22}$$

$$\begin{bmatrix} a_x \\ a_y \\ a_z - g \end{bmatrix}_{W,r} = \begin{bmatrix} \cos\Phi\sin\Theta \\ \sin\Phi \\ \cos\Phi\cos\Theta \end{bmatrix} \cdot f_z \tag{23}$$

Solving the pitch and bank angles, the reference rotation matrix can be expressed by the reference acceleration,

$$\boldsymbol{M}_{WB,r} = \begin{bmatrix} \frac{a_z - g}{a_{xz}} & \frac{a_x a_y}{a_{xz} f_z} & \frac{a_x}{f_z} \\ 0 & \frac{a_{xz}}{f_z} & \frac{a_y}{f_z} \\ -\frac{a_x}{a_{xz}} & \frac{a_x a_y}{a_{xz} f_z} & \frac{a_z - g}{f_z} \end{bmatrix} \tag{24}$$

Where,

$$\begin{cases} f_z = -\sqrt{a_x^2 + a_y^2 + (a_z - g)^2} \\ a_{xz} = -\sqrt{a_x^2 + (a_z - g)^2} \end{cases} \tag{25}$$

In the implementation, singularities at $f_z = 0$ and $a_{xz} = 0$ can be easily avoided by bounding a_z away from g.

2.3 Error Controller

The linear error controller mainly accounts for inversion errors and external disturbances. In addition, the state limits should also be applied to the state commands, similar with that of the reference model.

The control law is normally designed as,

$$v = \dddot{\vec{a}}_c = \dddot{\vec{a}}_r + k_3(\ddot{\vec{a}}_r - \ddot{\vec{a}}) + k_2(\dot{\vec{a}}_r - \dot{\vec{a}}) + k_1(\vec{v}_r - \vec{v}) + k_0(\vec{r}_r - \vec{r}) \tag{26}$$

We can calculate the transform function from the reference signal to the state output, assuming perfect plant model and ignoring actuator dynamics,

$$\vec{r} = \frac{s^4 + k_3 s^3 + k_2 s^2 + k_1 s + k_0}{s^4 + k_3 s^3 + k_2 s^2 + k_1 s + k_0} \vec{r}_r \tag{27}$$

Similar with the reference model modification, we can rewrite the control law into the following form. One thing differs from the reference model is the feedforward reference commands.

$$\dddot{\vec{a}}_c = \dddot{\vec{a}}_r + k_3 \left\{ \underbrace{\frac{k_2}{k_3} \left\{ \underbrace{\frac{k_1}{k_2} \left[\underbrace{\frac{k_0}{k_1}(\vec{r}_r - \vec{r}) + \vec{v}_r}_{\vec{v}_c} - \vec{v} \right]}_{\vec{a}_c} + \vec{a}_r - \vec{a} \right\}}_{\ddot{\vec{a}}_c} + \ddot{\vec{a}}_r - \ddot{\vec{a}} \right\} \tag{28}$$

$$\begin{cases} \vec{\boldsymbol{v}}_{\boldsymbol{c}} = \frac{k_0}{k_1}(\vec{\boldsymbol{r}}_r - \vec{\boldsymbol{r}}) + \vec{\boldsymbol{v}}_r \\ \vec{\boldsymbol{a}}_{\boldsymbol{c}} = \frac{k_1}{k_2}(\vec{\boldsymbol{v}}_{\boldsymbol{c}} - \vec{\boldsymbol{v}}) + \vec{\boldsymbol{a}}_r \\ \dot{\vec{\boldsymbol{a}}}_{\boldsymbol{c}} = \frac{k_2}{k_3}(\vec{\boldsymbol{a}}_{\boldsymbol{c}} - \vec{\boldsymbol{a}}) + \dot{\vec{\boldsymbol{a}}}_r \\ \ddot{\vec{\boldsymbol{a}}}_c = k_3\left(\dot{\vec{\boldsymbol{a}}}_c - \dot{\vec{\boldsymbol{a}}}\right) + \ddot{\vec{\boldsymbol{a}}}_r \end{cases} \tag{29}$$

In the above equation, the reference signals are within the state limitations, but not the error feedback signals. So in order to avoid giving out-of-bound commands due to the error dynamics, similar technique with the reference model should be applied here again, specifically on $\vec{\boldsymbol{v}}_{\boldsymbol{c}}$, $\vec{\boldsymbol{a}}_{\boldsymbol{c}}$ and $\dot{\vec{\boldsymbol{a}}}_{\boldsymbol{c}}$. The velocity command can be directly limited while the $\vec{\boldsymbol{a}}_{\boldsymbol{c}}$ and $\dot{\vec{\boldsymbol{a}}}_{\boldsymbol{c}}$ is converted to the commanded thrust and angular rate using Eqs. (18) and (19). Then limits are applied according to their physical constraints, and afterwards they are converted back to the linear state commands.

To provide good accuracy and robustness, pole placement method is used here for simple gain tuning, same as in Eq. (15),

$$\begin{cases} \frac{k_0}{k_1} = \frac{\omega}{4} \\ \frac{k_1}{k_2} = \frac{2\omega}{3} \\ \frac{k_2}{k_3} = \frac{3\omega}{2} \\ k_3 = 4\omega \end{cases} \tag{30}$$

2.4 4th Order Translational Dynamic Inversion

Eq. (13) gives the fourth derivative of the position. By inverting it, we have the following commands,

$$\begin{bmatrix} \dot{p} \\ \dot{q} \\ \ddot{T} \end{bmatrix}_c = \begin{bmatrix} 0 & T^{-1} & 0 \\ -T^{-1} & 0 & 0 \\ 0 & 0 & -1 \end{bmatrix} \left(\boldsymbol{M}_{BW} m \ddot{\vec{\boldsymbol{a}}} - \begin{bmatrix} -Trp - 2\dot{T}q \\ -Trq + 2\dot{T}p \\ Tp^2 + Tq^2 \end{bmatrix} \right) \tag{31}$$

In the implementation, the acceleration 2nd derivative $\ddot{\vec{\boldsymbol{a}}}$ is the pseudo control v resulting from the error controller. The thrust T can be approximated by $-mf_z$ from the accelerometer. Thrust derivative $\dot{T}$ is the only signal in the equation that doesn't have any measurement, but it can be approximated by filtering the motor thrust commands, where the filter is designed according to the motor dynamics.

$$\begin{bmatrix}\dot{p}\\ \dot{q}\\ \ddot{T}\end{bmatrix}_c = \begin{bmatrix}0 & -f_z^{-1} & 0\\ f_z^{-1} & 0 & 0\\ 0 & 0 & -1\end{bmatrix}\left(\boldsymbol{M}_{BW}\cdot v - \begin{bmatrix}f_z rp - \frac{2\dot{T}q}{m}\\ f_z rq + \frac{2\dot{T}p}{m}\\ -f_z p^2 - f_z q^2\end{bmatrix}\right) \tag{32}$$

After the translational dynamic inversion, the command pitch and bank rate accelerations then go to the rotational dynamic inversion and the thrust command is generated by integrating $\ddot{T}$ twice, as shown in Fig. 1.

$$T_c = \frac{1}{s^2}\ddot{T}_c \tag{33}$$

2.5 Heading Controller and Rotational Dynamic Inversion

Dynamic inversion control can be also applied to heading angle control, but singularity will be introduced [9].Considering the yaw dynamics are relatively slow and inherently decoupled from position dynamics for quadrotors, cascaded linear controller is enough for the control purpose.

$$\dot{r}_c = k_r[k_\Psi(\Psi_c - \Psi) - r] \tag{34}$$

The well-know rotational dynamic equation is,

$$\dot{\vec{\boldsymbol{\omega}}} = \boldsymbol{J}^{-1}\cdot\vec{\boldsymbol{M}} - \boldsymbol{J}^{-1}\cdot\vec{\boldsymbol{\omega}}\times\boldsymbol{J}\cdot\vec{\boldsymbol{\omega}} \tag{35}$$

Together with the pitch and roll angular accelerations commands from Eq. (32), the desired moments can be computed by inverting the rotational dynamic equation,

$$\vec{\boldsymbol{M}}_{\mathrm{c}} = \boldsymbol{J}\cdot\dot{\vec{\boldsymbol{\omega}}}_{\mathrm{c}} + \vec{\boldsymbol{\omega}}\times\boldsymbol{J}\cdot\vec{\boldsymbol{\omega}} \tag{36}$$

2.6 Control Allocation

The control allocation allocates the commanded total thrust and moments to the individual thrust of each motor, and then the RPM of each motor. Quadratic relationship is often assumed between the motor thrust and motor RPM. The mapping equations are,

$$\begin{bmatrix} L \\ M \\ N \\ T \end{bmatrix} = \begin{bmatrix} 0 & -R & 0 & R \\ R & 0 & -R & 0 \\ -k_m & k_m & -k_m & k_m \\ 1 & 1 & 1 & 1 \end{bmatrix} \begin{bmatrix} F_{prop,1} \\ F_{prop,2} \\ F_{prop,3} \\ F_{prop,4} \end{bmatrix} \tag{37}$$

$$\begin{cases} F_{prop,i} = k_n \cdot n_i^2 \\ M_{prop,i} = k_m \cdot F_{prop,i} \end{cases} \tag{38}$$

The normal control allocation equation is obtained by inverting the mapping equation using the thrust and moment commands,

$$\begin{bmatrix} F_{prop,1} \\ F_{prop,2} \\ F_{prop,3} \\ F_{prop,4} \end{bmatrix}_c = \frac{1}{4} \begin{bmatrix} 0 & 2R^{-1} & -k_m^{-1} & 1 \\ -2R^{-1} & 0 & k_m^{-1} & 1 \\ 0 & -2R^{-1} & -k_m^{-1} & 1 \\ 2R^{-1} & 0 & k_m^{-1} & 1 \end{bmatrix} \begin{bmatrix} L \\ M \\ N \\ T \end{bmatrix}_c \tag{39}$$

$$n_{i,c} = \sqrt{\frac{F_{prop,i,c}}{k_n}} \tag{40}$$

The above allocation works well in the nominal range. However, when there is not enough control power to provide enough thrust and moments simultaneously, priorities should be defined. Optimization is not necessary for quadcopter, as there is no redundancy in the system.

In general, the pitching and rolling moments have the top priorities as they control the direction of the thrust vector. After that the magnitude of the thrust vector has second priority, and last is the yawing moment.

Step 1, for the pitching and rolling moments only the hardware limit is imposed,

$$\begin{cases} -0.595 < L_c < 0.595 \\ -0.595 < M_c < 0.595 \end{cases} \tag{41}$$

Step 2, for the total thrust, not only the hardware limit is imposed, but also the pitching and rolling moments limits are considered. By imposing the limits, the total thrust is dynamically limited by the pitching and rolling moments.

$$\begin{cases} 0.4 < T_c < 14 \\ max\left(\left|\frac{2L_c}{R}\right|, \left|\frac{2M_c}{R}\right|\right) < T_c < 14 - max\left(\left|\frac{2L_c}{R}\right|, \left|\frac{2M_c}{R}\right|\right) \end{cases} \tag{42}$$

Step 3, for the yawing moments, the limits comes from the physical limits and the other three control inputs

$$\begin{cases} -0.112 < N_c < 0.112 \\ max\left(\left|\frac{2L_c}{R}\right| - T_C, T_C + \left|\frac{2M_c}{R}\right| - 14\right) < \frac{N_c}{k_m} < min\left(T_c - \left|\frac{2M_c}{R}\right|, 14 - T_C - \left|\frac{2L_c}{R}\right|\right) \end{cases} \tag{43}$$

2.7 Pseudo Control Hedging

Pseudo Control Hedging (PCH) is implemented to 'hide' the actuator dynamics from the error dynamics [10]. The expected reaction of the plant, acceleration 2nd derivative $\hat{v}$ is calculated using Eqs.(38), (37), (35), and (13), in which the each individual motor thrust and the thrust 2nd derivative are the inputs. As the inputs are not measureable, they are estimated by filtering the commanded inputs and the filters are designed according to the modeled actuator dynamics. In our case, it is a second order low pass filter. Then the hedging signal or the expected reaction deficit can be calculated by subtracting the expected reaction with the pseudo control,

$$v_h = v - \hat{v} \tag{44}$$

The dynamics of the reference model can be then decelerated by the expected reaction deficit. Another function of PCH is to prevent the integrator wind-up in the error dynamics [10] and parameter burst in the adaptive estimation.

3. L1 Adaptive Augmentation

One distinct advantage of combined design of baseline controller plus adaptive augmentation is that the adaptive controller doesn't need to care about desired dynamics or the system matrix, because it has been assigned properly by the baseline controller, which can make good use of the known plant knowledge. The L1 adaptive controller only needs to compensate for plant uncertainties including inversion error, disturbances and parameter changes. However, if very little plant knowledge is known, full adaptive controller maybe be more appropriate, such as in the work [13] where a L1 adaptive attitude controller was developed.

In this design, the L1 adaptive controller is implemented on the rotational dynamics, based on the following two reasons,

1. Most of the quadrotor uncertainties appear in the rotational dynamics and control allocation. And those are matched uncertainties.
2. The best available sensor on the quad is often the gyroscope. Other conventional sensors include accelerometer, pressure sensor, magnetometer and GPS, which are either very noisy or with bad accuracy.

First let's recall the dynamic equations from the angular accelerations $\dot{\vec{\omega}}$ to the system RPM inputs,

$$\dot{\vec{\omega}} = \boldsymbol{J}^{-1}\vec{\mathrm{M}} - \boldsymbol{J}^{-1}\vec{\omega} \times \boldsymbol{J} \cdot \vec{\omega} \tag{45}$$

$$\begin{bmatrix} L \\ M \\ N \end{bmatrix} = \begin{bmatrix} 0 & -R & 0 & R \\ R & 0 & -R & 0 \\ -k_m & k_m & -k_m & k_m \end{bmatrix} \begin{bmatrix} k_n \cdot n_1^2 \\ k_n \cdot n_2^2 \\ k_n \cdot n_3^2 \\ k_n \cdot n_4^2 \end{bmatrix} \tag{46}$$

We can rewrite them in the following form,

$$\begin{bmatrix} L \\ M \\ N \end{bmatrix} = \underbrace{\begin{bmatrix} k_n \cdot R & 0 & 0 \\ 0 & k_n \cdot R & 0 \\ 0 & 0 & k_m \end{bmatrix}}_{\boldsymbol{K_{mn}}} \underbrace{\begin{bmatrix} n_4^2 - n_2^2 \\ n_1^2 - n_3^2 \\ n_2^2 + n_4^2 - n_1^2 - n_3^2 \end{bmatrix}}_{\boldsymbol{u_n}} = \boldsymbol{K_{mn}} \cdot \boldsymbol{u_n} \tag{47}$$

$$\dot{\vec{\omega}} = \boldsymbol{J^{-1}} \cdot \boldsymbol{K_{mn}} \cdot \boldsymbol{u_n} - \boldsymbol{J^{-1}} \cdot \vec{\omega} \times \boldsymbol{J} \cdot \vec{\omega} \tag{48}$$

In the control allocation and rotational dynamic inversion, the system inputs are computed from the commanded angular acceleration $\dot{\vec{\omega}}_c$ and use the estimated parameters (denoted with hat),

$$\boldsymbol{u_n} = \boldsymbol{\hat{K}_{mn}^{-1}}\left(\hat{\boldsymbol{J}} \cdot \dot{\vec{\omega}}_c + \vec{\omega} \times \hat{\boldsymbol{J}} \cdot \vec{\omega}\right) \tag{49}$$

$$\boldsymbol{\hat{K}_{mn}^{-1}} = \begin{bmatrix} \hat{k}_n^{-1} \cdot R^{-1} & 0 & 0 \\ 0 & \hat{k}_n^{-1} \cdot R^{-1} & 0 \\ 0 & 0 & \hat{k}_m^{-1} \end{bmatrix} \tag{50}$$

Substitute the above equation in the dynamic equation in Eq. (48),

$$\dot{\vec{\omega}} = \boldsymbol{J^{-1}K_{mn}\hat{K}_{mn}^{-1}}\left(\hat{\boldsymbol{J}} \cdot \dot{\vec{\omega}}_c + \vec{\omega} \times \hat{\boldsymbol{J}} \cdot \vec{\omega}\right) - \boldsymbol{J^{-1}} \cdot \vec{\omega} \times \boldsymbol{J} \cdot \vec{\omega} \tag{51}$$

$$\dot{\vec{\omega}} = \boldsymbol{J^{-1}K_{mn}\hat{K}_{mn}^{-1}\hat{J}} \cdot \dot{\vec{\omega}}_c + \boldsymbol{J^{-1}}\left(\boldsymbol{K_{mn}\hat{K}_{mn}^{-1}} \cdot \vec{\omega} \times \hat{\boldsymbol{J}} \cdot \vec{\omega} - \vec{\omega} \times \boldsymbol{J} \cdot \vec{\omega}\right) \tag{52}$$

We can summarize the uncertainties together,

$$\dot{\vec{\omega}} = \dot{\vec{\omega}}_c + \Delta\vec{\boldsymbol{f}}_{\boldsymbol{\omega}} \tag{53}$$

$$\Delta\vec{\boldsymbol{f}}_{\boldsymbol{\omega}} = \left(\boldsymbol{J^{-1}K_{mn}\hat{K}_{mn}^{-1}\hat{J}} - \boldsymbol{I}\right)\dot{\vec{\omega}}_c + \boldsymbol{J^{-1}}\left(\boldsymbol{K_{mn}\hat{K}_{mn}^{-1}} \cdot \vec{\omega} \times \hat{\boldsymbol{J}} - \vec{\omega} \times \boldsymbol{J}\right)\vec{\omega} \tag{54}$$

The L1 adaptive element should estimate the uncertainties $\Delta\vec{\boldsymbol{f}}_{\boldsymbol{\omega}}$ and augment the baseline control $\dot{\vec{\omega}}_b$ by an adaptive control $\dot{\vec{\omega}}_a$ for the commanded angular acceleration. The baseline control gives the desired dynamics and the adaptive control compensates the uncertainties.

$$\dot{\vec{\omega}}_c = \dot{\vec{\omega}}_b + \dot{\vec{\omega}}_a \tag{55}$$

To estimate the $\Delta\vec{\boldsymbol{f}}_{\boldsymbol{\omega}}$, the following state predictor is considered,

$$\dot{\hat{\bar{\omega}}} = \dot{\bar{\omega}}_c + \Delta\hat{\vec{\boldsymbol{f}}}_{\boldsymbol{\omega}} + \boldsymbol{K_{sp}}\tilde{\bar{\omega}} \tag{56}$$

Where the prediction error and parameter error is defined as

$$\begin{cases} \tilde{\vec{\boldsymbol{\omega}}} = \hat{\vec{\boldsymbol{\omega}}} - \vec{\boldsymbol{\omega}} \\ \Delta\tilde{\vec{\boldsymbol{f}}}_{\boldsymbol{\omega}} = \Delta\hat{\vec{\boldsymbol{f}}}_{\boldsymbol{\omega}} - \Delta\vec{\boldsymbol{f}}_{\boldsymbol{\omega}} \end{cases} \tag{57}$$

The error dynamics can be derived by subtracting Eq. (57) by Eq. (53),

$$\dot{\tilde{\vec{\boldsymbol{\omega}}}} = \Delta\tilde{\vec{\boldsymbol{f}}}_{\boldsymbol{\omega}} + \boldsymbol{K_{sp}}\tilde{\vec{\boldsymbol{\omega}}} \tag{58}$$

Following a similar argument as in Section 3.3 of [14], one can derive the update law of piecewise constant type,

$$\Delta\hat{\vec{\boldsymbol{f}}}_{\boldsymbol{\omega}} = \left(1 - e^{\boldsymbol{K_{sp}}T_S}\right)^{-1}\boldsymbol{K_{sp}}e^{\boldsymbol{K_{sp}}T_S}\tilde{\vec{\boldsymbol{\omega}}} \tag{59}$$

Where T_s is the adaptation update rate, which is limited by the hardware constraints [10]. In our quadrotor case, it is 1 millisecond. The adaptive control law is,

$$\dot{\vec{\boldsymbol{\omega}}}_a = -C(s)\Delta\hat{\vec{\boldsymbol{f}}}_{\boldsymbol{\omega}} \tag{60}$$

where $C(s)$ is a low pass transfer function. Its bandwidth is limited by the dynamic bandwidth of the quadrotor and thus designed accordingly.

4. Experiment Results

The control design is verified in an indoor stereo web-camera tracking system [7], which can provide 25 Hz position signal with accuracy about 10 cm and latency about 100 ms. The quadrotor used is the 'Hummingbird' from Ascending technology [15]. The flight test results are given in the following figure. However, there are motion blur problems at high speed flight due to the low update rate of the webcams. Hence, GPS flight test is planned to break the speed limit. GPS flight test data will be presented in the final version.

The position tracking results of the baseline dynamic inversion control is shown in Fig. 4(a-c). An 8-shape trajectory was commanded and the reference position signals can be precisely tracked at high bandwidth. One interesting aspect in the implementation is that the accelerometer measurements in the x-y-axis of Body frame need to be filtered and bounded, because the quadrotor compensates

the disturbing force in x-y-axis of Body frame by pitching down. For instance, when the quadrotor hits the wall or being pushed, the controller will try to over-come that by pitching down, and if the feedback is not bounded it will pitch over 90 degree. The feedback of x-y-axis accelerometer measurement is especially beneficial to account for aerodynamic drag and steady wind disturbance. In our case, they are filtered and bounded within $5m/s^2$, considering the aerodynamic drag at maximum cruise speed is $3-4m/s^2$.

The L1 adaptive control is demonstrated by hanging a 180g mass under one tip of the quadrotor arm and then cutting if off. both actions are during the flight. Considering the desired payload is only 200g, the mass add quite large moment to the quadrotor, almost 50% of the maximum actuated moment. The true adaptive control signal can be approximately computed,

$$\dot{\vec{\omega}}^{*}_{a,x} \approx \frac{\Delta mgR}{J_{xx}} \approx \frac{0.18 \cdot 9.81 \cdot 0.17}{0.005} = 60.04 \tag{61}$$

The augmented adaptive control signals are shown in Fig 4(d). We can clearly see the quick adaptation of the signals, especially when the hanging mass was cut off at 393s, the $\dot{\vec{\omega}}_{a,x}$ is adapted instantaneously to the true value and almost no transient behavior can be observed.

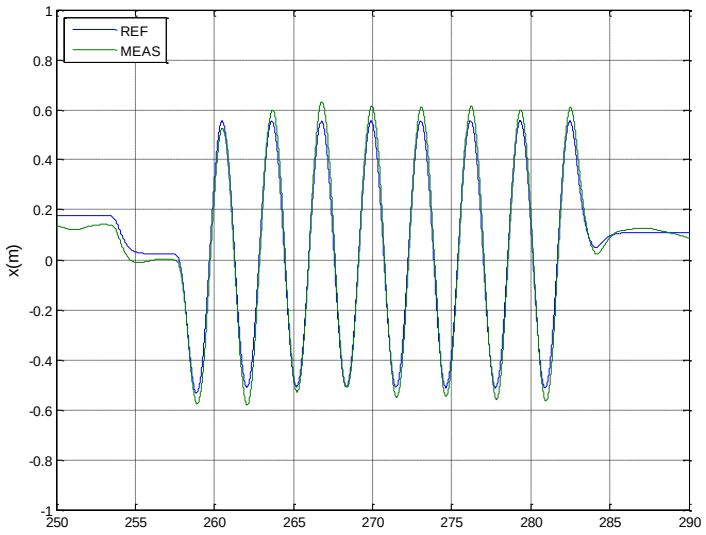

(a) Position Tracking in x axis

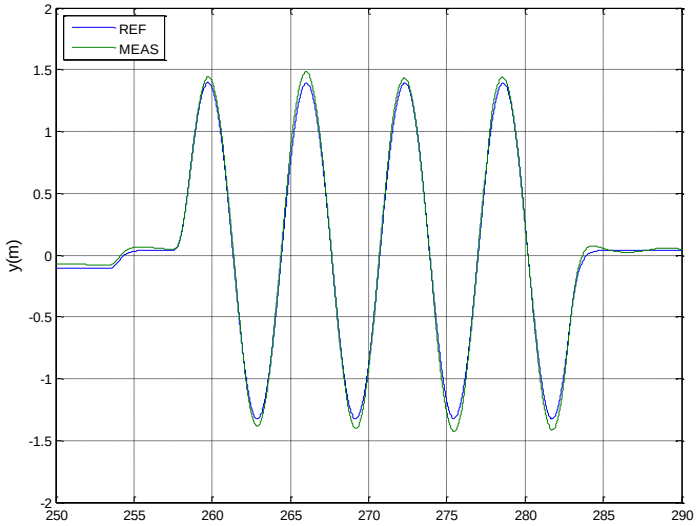

(b) Position Tracking in y axis

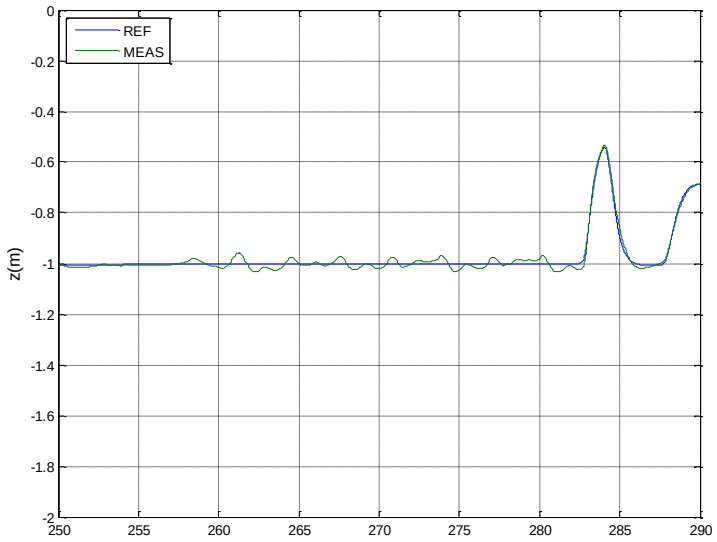

(c) Position Tracking in z axis

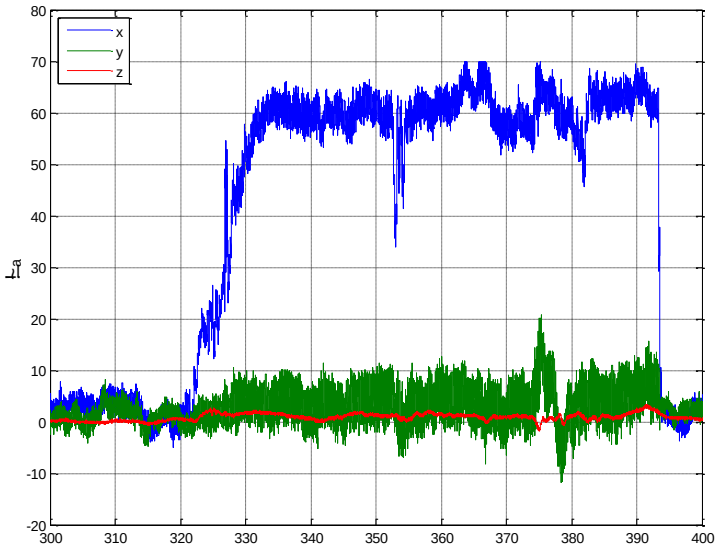

(d) L1 Augmented adaptive control $\dot{\boldsymbol{\omega}}_a$

Fig. 4. Experimental Results

5. Conclusion

The designed position controller can give the best bandwidth to the position control. And the dynamic inversion equation is extremely efficient without any linear approximation. The technique to incorporate the nonlinear state limitations in the reference model and error controller can prevent out-of-bound commands to the plant and thus increase the robustness of the control system.

The augmented L1 adaptive control compensates the system uncertainties, like inversion error, parameter changes and external disturbances.

6. Acknowledgments

J.W. Author gratefully acknowledges the support of the Technische Universität München – International Graduate School of Science and Engineering (IGSSE) and Institute for Advanced Study, funded by the German Excellence Initiative, project 4.03 Image Aided Flight Control.

Reference

1. Mellinger D, Michael N, and Kumar V (2012) Trajectory Generation and Control for Precise Aggressive Maneuvers with Quadrotors. International Journal of Robotics Research
2. Lupashin S, Andrea R D (2011) Adaptive Open-Loop Aerobatic Maneuvers for Quadrocopters. IFAC World Congress, pp. 2600–2606
3. Vicon Motion System. http://www.vicon.com. Accessed 13 July 2012
4. Wang, J, Holzapfel F (2013) Comparison of Dynamic Inversion and Backstepping Controls with application to a quadrotor. CEAS EuroGNC, Delft
5. Buhl M, Fritsch O, Lohmann B (2011) Exakte Ein-/Ausgangslinearisierung für die translatorische Dynamik eines Quadrocopters. Automatisierungstechnik, Vol. 59, Issue 6, pp. 374-381
6. Mistler V, Benallegue A, and M'Sirdi N K (2001) Exact linearization and noninteracting control of a 4 rotors helicopter via dynamic feedback," Proceedings 10th IEEE International Workshop on Robot and Human Interactive Communication. ROMAN (Cat. No.01TH8591), pp. 586-593
7. Klose S, Wang, J et al (2010) Markerless Vision Assisted Flight Control of a Quadrocopter. IEEE 2010, RSJ International Conference on Intelligent Robots and Systems
8. Wang J, Bierling T et al (2011) Novel Dynamic Inversion Architecture Design for Quadrocopter Control. 'Advances in Aerospace Guidance, Navigation and Control', F. Holzapfel and S. Theil, Eds. Springer Berlin Heidelberg, pp. 261-272
9. Wang J, Raffler T, and Holzapfel F (2012) Nonlinear Position Control Approaches for Quadcopters Using a Novel State Representation. AIAA Guidance, Navigation and Control Conference, Minneapolis, AIAA-2012-4913
10. Johnson E (2000) Limited Authority Adaptive Flight Control, PhD thesis, Georgia Institute of Technology
11. Hovakimyan, N, Cao, C (2010) L1 Adaptive Control Theory: guaranteed robustness with fast adaptation, SIAM, Philadelphia
12. Khalil H (2002) Feedback linearization in: Nonlinear Systems, 3rd ed. Prentice Hall
13. Mallikarjunan S. (2012) L 1 Adaptive Controller for Attitude Control of Multirotors, in AIAA Guidance, Navigation and Control Conference, Minneapolis, MN, AIAA-2012-4831
14. Kharisov E, Hovakimyan N, and Karl J (2010) Comparison of Several Adaptive Controllers According to Their Robustness Metrics. AIAA Guidance, Navigation and Control Conference, Toronto, Canada, AIAA-2010-8047
15. Ascending technologies GmbH, Hummingbird Quadrotor. http://www.asctec.de. Accessed 27 July 2010